Δ40p53 plays a distinct regulatory role in maintaining cellular homeostasis by controlling SGSH expression via miR-4651-5p

Apala Pal[1], Pritam Kumar Ghosh[1], Sahana Ghosh[2], Sachin Kumar Tripathi[1], Subrata Patra[2], Debjit Khan[1,6], Arindam Maitra[2] and Saumitra Das[1, *]

[1]Department of Microbiology and Cell Biology, Indian Institute of Science, Bangalore-560012, India.
[2]National Institute of Biomedical Genomics, Kalyani-741251, India.
[6]Department of Life Sciences, GITAM School of Science, GITAM (Deemed to be University), Bangalore-562163, India.

*Address for correspondence:

Dr. Saumitra Das, Professor,
Department of Microbiology and Cell Biology,
Indian Institute of Science, Bangalore-560012, India
Email: sdas@iisc.ac.in
Phone: 91 80 2293 2886
Fax: 91 80 2360 2697

ABSTRACT

Δ40p53, the only translational isoform of p53, modulates the full-length p53 (FLp53) activity and independently regulates targets such as the miR-186-5p–YY1 axis. To identify additional miRNAs regulated by Δ40p53, we performed small RNA sequencing. We found that overexpression of Δ40p53, but not FLp53, significantly downregulated miR-4671-5p. Expression of both isoforms at varying ratios revealed that miR-4671-5p may be modulated by FLp53 in a Δ40p53-dependent manner. *In silico* analysis identified SGSH (N-sulfoglucosamine sulfohydrolase) as a potential miR-4671-5p target. SGSH expression showed inverse correlation with miR-4671-5p in cancer datasets and prognostic significance. SGSH mRNA and protein levels were reduced upon miR-4671-5p overexpression or siΔ40p53 treatment, confirming regulatory linkage. Functionally, miR-4671-5p overexpression induced intra-S-phase cell cycle arrest, implicating SGSH in cell cycle regulation. These results reveal a novel Δ40p53–miR-4671-5p–SGSH axis that impacts cell cycle progression and may contribute to cancer outcomes. Our findings highlight the distinct regulatory role of Δ40p53, independent of FLp53, in maintaining cellular and metabolic homeostasis via miRNA-mediated mechanisms.

Keywords: p53 isoform, Δ40p53 role, miR-4671-5p expression, SGSH role in cell cycle regulation

INTRODUCTION

Genome integrity relies on rapid recognition and repair of DNA damage. Central to this response is p53, which halts the cell cycle, limits proliferation of damaged cells, and is frequently inactivated by mutation in cancer (Kops et al., 2005; Rivlin et al., 2011). p53 activity is further shaped by 12 naturally occurring isoforms that differ at the N- and C-termini (Bourdon, 2007; Khoury & Bourdon, 2011). Their relative abundance varies across normal tissues and tumours, altering transcriptional output and cellular fate (Bourdon et al., 2005; Vieler & Sanyal, 2018). Δ40p53 is the sole translational isoform, produced from an internal ribosome-entry site (IRES) within the TP53 5′-UTR (Ray et al., 2006). A second IRES yields full-length p53 (FLp53); the two proteins share oligomerisation domains and form homo- and hetero-tetramers (Ghosh et al., 2004). IRES usage is stress- and cell-cycle-phase dependent: translation of FLp53 peaks at the G2/M transition, whereas Δ40p53 is preferentially produced at G1/S (Ray et al., 2006; Khan et al., 2015).

Functionally, Δ40p53 fine-tunes FLp53 activity yet also acts independently. It retains the second transactivation domain of p53, driving gene expression in p53-null cells (Maier et al., 2004; Ohki et al., 2007). Reported activities include induction of 14-3-3σ and G2 arrest (Bourougaa et al., 2010), activation of pro-apoptotic BAX and GADD45 (Steffens Reinhardt et al., 2020), modulation of the Nanog–IGF1 axis during stem-cell differentiation (Ungewitter & Scrable, 2010), and control of β-cell proliferation and glucose homeostasis (Hinault et al., 2011). At baseline, Δ40p53 and FLp53 suppress migration and proliferation in breast cancer (Zhang et al., 2022). Conversely, Δ40p53 can promote survival by transactivating netrin-1 (Sun et al., 2021). Growing evidence links Δ40p53 to non-coding RNA networks. We previously showed that Δ40p53—but not FLp53—up-regulates miR-186-5p, which represses the oncogenic transcription factor YY1 and limits proliferation (Katoch et al., 2021). Δ40p53 also controls the lncRNA LINC00176, influencing multiple miRNAs and mRNAs that govern cell fate (Pal et al., 2023). These findings suggest that isoform-specific miRNA programmes are key to Δ40p53 function, yet a systematic catalogue of such miRNAs is lacking.

We performed small-RNA sequencing to globally identify miRNAs differentially regulated by Δ40p53 and FLp53. Using lung (H1299) and colon (HCT116) cancer cell lines engineered to express FLp53, Δ40p53, or both, we discovered miR-4671-5p as a Δ40p53-specific target. Down-stream analyses revealed its repression of N-sulfoglucosamine sulfohydrolase (SGSH), linkage to S-phase arrest, and prognostic significance in multiple tumours. Here, we delineate the Δ40p53–miR-4671-5p–SGSH axis and its impact on cell-cycle control, providing fresh insight into isoform-specific p53 signalling.

MATERIALS AND METHODS

Cell lines and transfections

Three human cell lines were used: H1299 (lung adenocarcinoma, p53-null), HCT116 p53+/+ (referred to as HCT116+/+), and HCT116 p53–/– (referred to as HCT116–/–), which endogenously expresses only Δ40p53. Cells were cultured in Dulbecco's Modified Eagle Medium (DMEM, Sigma) supplemented with 10% fetal bovine serum (FBS, GIBCO, Invitrogen) and 1% penicillin/streptomycin. Transfections were performed using Lipofectamine 2000 and Turbofectamine (Invitrogen) in Opti-MEM (GIBCO) according to the manufacturer's instructions. After 4 hours, transfection medium was replaced with complete DMEM, and cells were harvested at indicated time points.

Plasmid constructs included pGFP-hp-p53-5′UTR vectors expressing FLp53, Δ40p53, or both (14A). These were generously provided by Dr. Robin Fahraeus (INSERM, France). To overexpress miR-4671-5p, the mature sequence was cloned into the pSUPER vector. For knockdown studies, a 30 nM siRNA targeting the 3′UTR of TP53 (IDT) was used, which downregulates both FLp53 and Δ40p53; a non-targeting control siRNA (Dharmacon) was used in parallel.

Small RNA Sequencing

RNA extraction: Total RNA was isolated from H1299 cells transfected with vector, FL p53, Δ40p53, or 14A using TRIzol followed by the PureLink kit (Ambion). RNA quality (Bioanalyzer 2100, Agilent) and quantity (NanoDrop, Qubit) were assessed; only samples with RIN > 7 were used for library preparation.

Library preparation and sequencing: One µg of high-quality RNA was processed with the Illumina TruSeq Small RNA kit. 3′/5′ adapters were ligated, cDNA was synthesised, PCR-amplified, and fragments of 145–160 bp were gel-purified. Libraries were pooled and sequenced (1 × 50 bp) on an Illumina HiSeq-2500.

RNA-seq data analysis: FASTQ files were trimmed with Cutadapt v1.8.1 and mapped to hg19 using miRDeep2. Known and novel miRNAs were quantified as reads-per-million (RPM); multi-precursor miRNAs were averaged. Differential expression was determined with DESeq2.

Western Blot analysis

Cells were lysed in RIPA buffer, and protein concentrations were determined via the Bradford assay. Equal amounts of lysate were resolved by SDS-PAGE and transferred to nitrocellulose membranes. Primary antibodies used were: anti-p53 (CM1; kindly provided by Dr. Robin Fahraeus (INSERM, France) and Prof. J.C. Bourdon (University of Dundee, UK), anti-SGSH (Abclonal A8148), anti-CDK11B (Ablconal A12830), and anti-CDK5R1 (Ablconal A14497). Blots were developed using HRP-conjugated secondary antibodies (Sigma) and detected with enhanced chemiluminescence (ECL).

RNA isolation and Real-time PCR

Total RNA was extracted using TRI Reagent™ (Sigma) and treated with DNase I (Promega) to remove DNA contamination. RNA was purified by acidic phenol–chloroform extraction and

ethanol precipitation, then quantified using a Nano-spectrophotometer. cDNA was synthesized from 2–5 µg total RNA for mRNAs or 50 ng for miRNAs using gene-specific primers and Revertaid™ MMLV RT (Thermo Scientific) at 42 °C for 1 hour.

Cell cycle Analysis

HCT116–/– cells were transfected with miR-4671-5p or miR-34a-5p overexpression constructs. After 48 h, cells were fixed in methanol, treated with RNase A (10 µg/mL), stained with propidium iodide (1 µg/mL), and analyzed on a BD FACSCalibur flow cytometer.

Bioinformatics and statistics

dbDEMC2.0 has been used to perform a meta-profiling of selected miRNAs (Xu et al., 2022). TargetScan 7.2 has been used to predict target mRNAs of miRNAs (Agarwal et al., 2015). miRDB has been used to predict target miRNAs (Chen and Wang, 2020; Liu and Wang, 2019). GO-term analysis was done on PANTHER release 17.0. Kaplan-Meier survival analysis was done on R2: Genomics Analysis and Visualization Platform. Heat map for Figure 1E has been generated using Heatmapper. Data were analyzed using two-tailed Student's t-test; $p \leq 0.05$ (*) or $p \leq 0.01$ (**) or $p \leq 0.001$(***)

RESULTS

Small RNA sequencing reveals miRNA targets of p53 and Δ40p53

H1299 cells, which lack endogenous p53 isoforms, were transfected to express FLp53, Δ40p53, both isoforms (14A), or GFP (control) **(Figure 1A–C).** Total RNA was extracted, quality-checked, and subjected to small RNA sequencing. From the dataset, 135 miRNAs with consistent unidirectional fold changes across replicates were selected. A heatmap visualized their expression profiles under each isoform condition **(Figure 1D)**. A statistically significant cluster of differentially expressed miRNAs ($p \leq 0.05$) was identified **(Figure 1E)**. Among these, four miRNAs stood out for their isoform-specific regulation. miR-4671-5p was significantly downregulated by Δ40p53 but unaffected by FLp53. In contrast, miR-301b-5p was reduced only in FLp53-expressing cells. miR-34a-5p, a known p53 target (Zhang et al., 2019) was upregulated in all isoform conditions and served as a positive control. Similarly, miR-548ae-5p was upregulated across FLp53, Δ40p53, and 14A conditions, indicating potential co-regulation. These results reveal distinct and overlapping miRNA regulatory profiles for FLp53 and Δ40p53, with miR-4671-5p emerging as a prominent Δ40p53-specific target for further investigation.

Selection and validation of miRNAs for further studies

To validate small RNA sequencing results, H1299 cells were transfected with FLp53, Δ40p53, 14A (both isoforms), or control vector (**Figure 2A**), and miRNA levels were measured by qRT-PCR. miR-4671-5p was significantly downregulated by Δ40p53 and 14A, but not by FLp53

alone (**Figure 2B**). In contrast, miR-34a-5p and miR-548ae-5p were consistently upregulated across all isoform conditions (**Figure 2C–D**). miR-301b-5p showed mild induction by Δ40p53 and 14A, but not FLp53 (**Figure 2E**). Expression patterns for miR-4671-5p, miR-548ae-5p, and miR-34a-5p matched the sequencing data (**Figure 2F**); miR-301b-5p was excluded from further analysis.

To assess physiological relevance, we examined these miRNAs in colon cancer cell lines HCT116+/+ (predominantly FLp53) and HCT116–/– (only Δ40p53) (**Figure 2G**). At baseline, HCT116–/– cells showed lower miR-4671-5p and higher miR-548ae-5p and miR-34a-5p levels than HCT116+/+ cells (**Figure 2H**). siRNA-mediated knockdown of p53 in HCT116+/+ cells reduced miR-548ae-5p and miR-34a-5p but did not significantly affect miR-4671-5p (**Figure 2I–J**). Conversely, Δ40p53 knockdown in HCT116–/– cells increased miR-4671-5p and decreased miR-548ae-5p and miR-34a-5p (**Figure 2K–L**). These results suggest that Δ40p53 specifically suppresses miR-4671-5p and enhances miR-548ae-5p and miR-34a-5p expression, while FLp53 does not regulate miR-4671-5p.

Given that p53 isoform expression varies widely across cancer types (Vieler and Sanyal, 2018), we next examined whether the expression patterns of these miRNAs—particularly miR-4671-5p—also show variability in clinical samples. To explore this, we analyzed publicly available cancer transcriptome datasets.

Regulation of miRNAs by Δ40p53 and p53

Bioinformatic analysis using dbDEMC 2.0 revealed that miR-34a-5p is widely expressed in many cancers, while miR-4671-5p expression is restricted to colon, lung, and pancreatic cancers. In contrast, miR-548ae-5p was undetectable in this dataset (**Figure 3A**). These observations suggest that the differential expression of these miRNAs may reflect the tissue-specific abundance of p53 and Δ40p53. To test this, we overexpressed p53 and Δ40p53 in varying ratios in H1299 cells and analyzed miRNA expression (**Figure 3B**). Expression of miR-34a-5p was induced by either isoform alone; however, certain combinations of both isoforms reduced its expression, suggesting dose-dependent co-regulation (**Figure 3C**), consistent with previous reports of p53/Δ40p53 interactions (Ghosh et al., 2004).

Notably, FLp53 overexpression alone did not significantly affect miR-4671-5p levels, whereas increasing Δ40p53 expression—either alone or in combination—consistently suppressed it (**Figure 3D**). The 14A construct mimicked this effect, indicating that p53 may modulate Δ40p53-mediated regulation of miR-4671-5p but is not itself sufficient to alter its expression. These data reinforce that Δ40p53 is the primary regulator of miR-4671-5p and that isoform balance is critical for miRNA output.

Cellular role of miR-4671-5p

Because miR-4671-5p was uniquely repressed by Δ40p53, we explored its downstream functions. TargetScan 7.2 and miRDB yielded 786 non-redundant putative targets, with GO enrichment for ‘protein-serine-kinase activity’ indicating that many predicted targets of miR-

168 4671-5p may be involved in cell cycle regulation. From this list we prioritised two cell-cycle
169 kinases, CDK11B and CDK5R1 for experimental follow-up (**Figure 3E; Figure S1**).
170 Additionally, we prioritized SGSH (N-sulfoglucosamine sulfohydrolase), the top-scoring
171 miR-4671-5p target in TargetScan, despite its uncharacterized role in cancer.

172 SGSH is a lysosomal enzyme whose deficiency causes mucopolysaccharidosis IIIA (MPS
173 IIIA), leading to GAG and heparan sulfate accumulation and resulting in severe neurological
174 and skeletal pathology (Li et al., 2018). Although SGSH has recently been linked to
175 monkeypox and interstitial lung disease (Anuraga et al., 2024; Ye et al., 2022), its role in tumor
176 biology remains unknown. Analysis of patient datasets revealed that low SGSH expression
177 correlates with poor survival in pancreatic cancer, while high SGSH is associated with poor
178 outcomes in colon tumors (**Figure 3F–I; Fig. S1, Table 3**). These trends are opposite to
179 miR-4671-5p levels observed in the same cancers (**Figure 3A**), suggesting a biologically
180 relevant interaction.

181 We next validated the regulation of these targets under varying p53/Δ40p53 expression in
182 H1299 cells. *SGSH*, *CDK11B*, and *CDK5R1* mRNA levels were upregulated only under
183 Δ40p53 overexpression (**Figure 3J–L**). Similarly, in HCT116–/– cells (expressing endogenous
184 Δ40p53), these proteins were more abundant than in HCT116+/+ cells (**Figure 3M**), consistent
185 with lower miR-4671-5p expression (**Figure 3A**). Partial knockdown of Δ40p53 reduced
186 expression of all three targets (**Figure 4A–B**), while overexpression of miR-4671-5p in
187 HCT116–/– cells led to reduced SGSH, CDK11B, and CDK5R1 mRNA levels, most
188 prominently for SGSH (**Figure 4C–D**). Corresponding decreases in SGSH protein were
189 observed under both conditions (**Figure 4E–F**).

190 Finally, miR-4671-5p overexpression caused significant S-phase accumulation and reduced
191 G2-phase cells, indicating intra-S phase arrest (Fig. 4G). Together, these findings establish that
192 Δ40p53 suppresses miR-4671-5p to maintain SGSH and other cell cycle regulators, enabling
193 proper S-phase progression.

194 **DISCUSSION**

195 MicroRNAs (miRNAs) play critical roles in regulating development, cell cycle progression,
196 and survival. Their dysregulation is a common feature in cancer (Israel et al., 2009). While
197 many miRNAs are known to be transcriptionally regulated by full-length p53 (FLp53) (Takwi
198 and Li, 2009), the contribution of p53 isoforms—especially Δ40p53—to miRNA regulation
199 has only recently been explored. We previously demonstrated that Δ40p53 selectively
200 upregulates miR-186-5p, which targets and represses the oncogene YY1, leading to reduced
201 cell proliferation (Katoch et al., 2021). Despite this, the full functional scope of Δ40p53
202 remains understudied, even though it has been implicated in key cellular processes such as
203 apoptosis, senescence, migration, and the cell cycle (Steffens Reinhardt et al., 2020). A key
204 open question is: which non-coding RNAs are specifically regulated by Δ40p53**,** and how
205 might these contribute to its distinct roles? This is particularly relevant in cancers, where

differential isoform expression (Vieler and Sanyal, 2018) may reshape downstream gene regulatory networks.

Here, we identified several miRNAs regulated by Δ40p53, either uniquely or in parallel with p53. Among these, miR-4671-5p was exclusively repressed by Δ40p53, prompting further investigation. Overexpression of Δ40p53 significantly reduced miR-4671-5p levels, whereas p53 alone had no effect. Interestingly, the dual-isoform construct (14A) also reduced miR-4671-5p expression (Figure 2B), suggesting that p53 may enhance Δ40p53-mediated repression. Similarly, varying p53/Δ40p53 ratios consistently decreased miR-4671-5p expression in the presence of both isoforms (Figure 3D). These findings indicate that relative isoform abundance modulates miR-4671-5p levels**,** which could contribute to context-dependent regulation of downstream targets in different cancers.

To explore the downstream role of miR-4671-5p, we initially selected SGSH, CDK11B, and CDK5R1 as candidate targets based on bioinformatic predictions and GO enrichment analysis (**Figure S1, Table 2**). Among these, SGSH was prioritized for further investigation due to its strong prediction score, metabolic function, and uncharacterized role in cancer. SGSH expression also showed prognostic significance: low SGSH associated with poor survival in pancreatic cancer, whereas high SGSH correlated with worse outcome in colon cancer, glioblastoma (**Figure 3F-I; Figure S1, Table 3**) and other datasets. Notably, SGSH and miR-4671-5p levels were inversely related across these tumours (**Figure 3A**), supporting functional linkage. The bidirectional prognostic pattern suggests SGSH is neither a classic oncogene nor tumour suppressor but may operate within tumour-specific rewiring of the Δ40p53–miR-4671-5p–SGSH axis—an area that merits deeper investigation.

Overexpression of Δ40p53 increased the mRNA levels of all three targets—SGSH, CDK11B, and CDK5R1 (**Figure 3J–L**)—with SGSH showing the **most pronounced upregulation**. Protein levels of all three were also higher in cells with endogenous Δ40p53 (**Figure 3M**). Although co-expression of FLp53 and Δ40p53 reduced miR-4671-5p levels (**Figure 3D**), this was not mirrored at the target mRNA level (**Figure 3J–L**), likely due to additional miRNAs regulated by the isoform combination influencing target expression. To validate the Δ40p53–miR-4671-5p–mRNA axis, we overexpressed miR-4671-5p or silenced Δ40p53, both of which led to reduced expression of all three targets, with **SGSH showing the most substantial decrease** (**Figure 4A, D**). This trend was confirmed at the protein level, where SGSH levels dropped consistently under both conditions (**Figure 4E, F**), highlighting SGSH as the **primary and most responsive target** within the Δ40p53–miR-4671-5p regulatory network.

To assess the physiological relevance of SGSH–miR-4671-5p regulation, we considered SGSH's established role in lysosomal degradation of heparan sulfate (HS), a glycosaminoglycan (Boado et al., 2018; Griffin and Gloster, 2017). In MPS Type IIIA, SGSH mutations impair this process, leading to intracellular accumulation of heparan sulfate. Notably, flow cytometry analyses in MPS models have revealed disrupted cell cycle profiles, including elevated S-phase and reduced G2-phase populations (Brokowska et al., 2022), suggesting a potential link between SGSH activity and cell cycle control.

Since CDK11B and CDK5R1—also miR-4671-5p targets—are known cell cycle regulators, we evaluated whether miR-4671-5p overexpression influenced cell cycle progression. We observed a significant increase in S-phase cells and a reduction in G2-phase cells (**Figure 4G**), indicative of intra-S-phase arrest. While this is consistent with the known roles of CDK11B and CDK5R1 in S–G2 transition, SGSH may also contribute to this effect through HS accumiation. Heparan sulfate accumulation is known to inhibit topoisomerase I, which disrupts DNA replication and induces intra-S-phase arrest (Kovalszky et al., 1998; Lin et al., 2014).

Thus, miR-4671-5p may induce intra-S arrest through dual mechanisms: direct repression of cell cycle kinases and indirect effects mediated by SGSH inhibition and subsequent glycosaminoglycan accumulation. However, the precise contribution of SGSH to this arrest phenotype—and its interaction with canonical cell cycle regulators—warrants further investigation to clarify its mechanistic role in this regulatory axis.

In conclusion, our study identifies a novel Δ40p53–miR-4671-5p–SGSH regulatory axis that contributes to maintaining proper cell cycle progression. Under physiological conditions, Δ40p53 suppresses miR-4671-5p, allowing sustained expression of SGSH and other cell cycle regulators such as CDK11B and CDK5R1, thereby supporting controlled S-phase progression. However, in pathological conditions where Δ40p53 levels are reduced, miR-4671-5p is derepressed, leading to downregulation of its targets and activation of intra-S-phase arrest. These findings emphasize the importance of isoform-specific p53 signaling in regulating non-coding RNA networks and suggest that alterations in Δ40p53 expression could have broad implications for cancer biology and potential therapeutic targeting (**Figure 4H**).

ACKNOWLEDGEMENTS

We thank Prof. J.C. Bourdon (University of Dundee) and Dr. Robin Fahraeus (INSERM) for the anti-p53 antibody. We acknowledge NIBMG (Kalyani, India) for RNA sequencing facilities and the SD lab members for helpful discussions. This work was supported by a DBT research grant to SD, who also received the J.C. Bose fellowship. Additional support came from the DBT-IISc partnership, DST-FIST Level II, and the UGC Centre of Advanced Studies.

AUTHOR CONTRIBUTIONS

AP and SD: Conception and design of studies analysis, interpretation, and article writing. AP, SKT and PKG: performing experiments, interpretation of results and article editing. DK: bioinformatic analysis, interpretation of results, article writing and editing. SaG, SP and AM: RNA sequencing and analysis. SD: Funding acquisition, supervision and project management.

DATA AVAILABILITY STATEMENT

The sequencing data files obtained is available in the online biorepository forum with the SRP BioProject ID **PRJEB47067.**

CONFLICT OF INTEREST

The authors declare no conflict of interest.

REFERENCE

Agarwal, V., Bell, G. W., Nam, J.-W. and Bartel, D. P. (2015). Predicting effective microRNA target sites in mammalian mRNAs. *Elife* **4**, e05005.

Anuraga, G., Lang, J., Xuan, D. T. M., Ta, H. D. K., Jiang, J. Z., Sun, Z., Dey, S., Kumar, S., Singh, A., Kajla, G. et al. (2024). Integrated bioinformatics approaches to investigate alterations in transcriptomic profiles of monkeypox infected human cell line model. *J Infect Public Health* **17**, 60-69.

Boado, R. J., Lu, J. Z., Hui, E. K.-W. and Pardridge, W. M. (2018). Reduction in Brain Heparan Sulfate with Systemic Administration of an IgG Trojan Horse–Sulfamidase Fusion Protein in the Mucopolysaccharidosis Type IIIA Mouse. *Molecular Pharmaceutics* **15**, 602-608.

Bourdon, J. C. (2007). p53 and its isoforms in cancer. *Br J Cancer* **97**, 277-82.

Bourdon, J. C., Fernandes, K., Murray-Zmijewski, F., Liu, G., Diot, A., Xirodimas, D. P., Saville, M. K. and Lane, D. P. (2005). p53 isoforms can regulate p53 transcriptional activity. *Genes Dev* **19**, 2122-37.

Bourougaa, K., Naski, N., Boularan, C., Mlynarczyk, C., Candeias, M. M., Marullo, S. and Fahraeus, R. (2010). Endoplasmic reticulum stress induces G2 cell-cycle arrest via mRNA translation of the p53 isoform p53/47. *Mol Cell* **38**, 78-88.

Brokowska, J., Gaffke, L., Pierzynowska, K., Cyske, Z. and Węgrzyn, G. (2022). Cell cycle disturbances in mucopolysaccharidoses: Transcriptomic and experimental studies on cellular models. *Exp Biol Med (Maywood)* **247**, 1639-1649.

Chen, Y. and Wang, X. (2020). miRDB: an online database for prediction of functional microRNA targets. *Nucleic Acids Res* **48**, D127-d131.

Ghosh, A., Stewart, D. and Matlashewski, G. (2004). Regulation of human p53 activity and cell localization by alternative splicing. *Mol Cell Biol* **24**, 7987-97.

Griffin, L. S. and Gloster, T. M. (2017). The Enzymatic Degradation of Heparan Sulfate. *Protein Pept Lett* **24**, 710-722.

Hafsi, H., Santos-Silva, D., Courtois-Cox, S. and Hainaut, P. (2013). Effects of Delta40p53, an isoform of p53 lacking the N-terminus, on transactivation capacity of the tumor suppressor protein p53. *BMC Cancer* **13**, 134.

Hinault, C., Kawamori, D., Liew, C. W., Maier, B., Hu, J., Keller, S. R., Mirmira, R. G., Scrable, H. and Kulkarni, R. N. (2011). Delta40 Isoform of p53 controls beta-cell proliferation and glucose homeostasis in mice. *Diabetes* **60**, 1210-22.

Israel, A., Sharan, R., Ruppin, E. and Galun, E. (2009). Increased MicroRNA Activity in Human Cancers. *PLoS One* **4**, e6045.

Katoch, A., Tripathi, S. K., Pal, A. and Das, S. (2021). Regulation of miR-186-YY1 axis by the p53 translational isoform Δ40p53: implications in cell proliferation. *Cell Cycle* **20**, 561-574.

Khan, D., Katoch, A., Das, A., Sharathchandra, A., Lal, R., Roy, P., Das, S., Chattopadhyay, S. and Das, S. (2015). Reversible induction of translational isoforms of p53 in glucose deprivation. *Cell Death Differ* **22**, 1203-18.

Khoury, M. P. and Bourdon, J. C. (2011). p53 Isoforms: An Intracellular Microprocessor? *Genes Cancer* **2**, 453-65.

Kops, G. J., Weaver, B. A. and Cleveland, D. W. (2005). On the road to cancer: aneuploidy and the mitotic checkpoint. *Nat Rev Cancer* **5**, 773-85.

Kovalszky, I., Dudás, J., Oláh-Nagy, J., Pogány, G., Töváry, J., Timár, J., Kopper, L., Jeney, A. and Iozzo, R. V. (1998). Inhibition of DNA topoisomerase I activity by heparan sulfate and modulation by basic fibroblast growth factor. *Mol Cell Biochem* **183**, 11-23.

329 **Li, X., Xiao, R., Chen, B., Yang, G., Zhang, X., Fu, Z., Fu, J., Zhuang, M. and Huang, Y.** (2018).
330 A novel mutation of SGSH and clinical features analysis of mucopolysaccharidosis type IIIA. *Medicine*
331 *(Baltimore)* **97**, e13758.
332 **Lin, R.-W., Yang, C.-N., Ku, S., Ho, C.-J., Huang, S.-B., Yang, M.-C., Chang, H.-W., Lin, C.-M.,**
333 **Hwang, J., Chen, Y.-L. et al.** (2014). CFS-1686 Causes Cell Cycle Arrest at Intra-S Phase by
334 Interference of Interaction of Topoisomerase 1 with DNA. *PLoS One* **9**, e113832.
335 **Liu, W. and Wang, X.** (2019). Prediction of functional microRNA targets by integrative
336 modeling of microRNA binding and target expression data. *Genome Biology* **20**, 18.
337 **Maier, B., Gluba, W., Bernier, B., Turner, T., Mohammad, K., Guise, T., Sutherland, A.,**
338 **Thorner, M. and Scrable, H.** (2004). Modulation of mammalian life span by the short isoform of p53.
339 *Genes Dev* **18**, 306-19.
340 **Ohki, R., Kawase, T., Ohta, T., Ichikawa, H. and Taya, Y.** (2007). Dissecting functional roles
341 of p53 N-terminal transactivation domains by microarray expression analysis. *Cancer Sci* **98**, 189-200.
342 **Ota, A., Nakao, H., Sawada, Y., Karnan, S., Wahiduzzaman, M., Inoue, T., Kobayashi, Y.,**
343 **Yamamoto, T., Ishii, N., Ohashi, T. et al.** (2017). Delta40p53alpha suppresses tumor cell proliferation
344 and induces cellular senescence in hepatocellular carcinoma cells. *J Cell Sci* **130**, 614-625.
345 **Pal, A., Ghosh, P. K. and Das, S.** (2023). The "LINC" between Δ40p53-miRNA Axis in the
346 Regulation of Cellular Homeostasis. *Mol Cell Biol* **43**, 335-353.
347 **Patil, P. S., Saklani, A., Gambhire, P., Mehta, S., Engineer, R., De'Souza, A., Chopra, S. and**
348 **Bal, M.** (2017). Colorectal Cancer in India: An Audit from a Tertiary Center in a Low Prevalence Area.
349 *Indian J Surg Oncol* **8**, 484-490.
350 **Powell, D. J., Hrstka, R., Candeias, M., Bourougaa, K., Vojtesek, B. and Fahraeus, R.** (2008).
351 Stress-dependent changes in the properties of p53 complexes by the alternative translation product
352 p53/47. *Cell Cycle* **7**, 950-9.
353 **Ray, P. S., Grover, R. and Das, S.** (2006). Two internal ribosome entry sites mediate the
354 translation of p53 isoforms. *EMBO Rep* **7**, 404-10.
355 **Rivlin, N., Brosh, R., Oren, M. and Rotter, V.** (2011). Mutations in the p53 Tumor Suppressor
356 Gene: Important Milestones at the Various Steps of Tumorigenesis. *Genes Cancer* **2**, 466-74.
357 **Sharathchandra, A., Katoch, A. and Das, S.** (2014). IRES mediated translational regulation of
358 p53 isoforms. *Wiley Interdiscip Rev RNA* **5**, 131-9.
359 **Steffens Reinhardt, L., Zhang, X., Wawruszak, A., Groen, K., De Iuliis, G. N. and Avery-**
360 **Kiejda, K. A.** (2020). Good Cop, Bad Cop: Defining the Roles of Delta40p53 in Cancer and Aging.
361 *Cancers (Basel)* **12**.
362 **Sun, Y., Manceau, A., Frydman, L., Cappuccio, L., Neves, D., Basso, V., Wang, H.,**
363 **Fombonne, J., Maisse, C., Mehlen, P. et al.** (2021). Delta40p53 isoform up-regulates netrin-1/UNC5B
364 expression and potentiates netrin-1 pro-oncogenic activity. *Proc Natl Acad Sci U S A* **118**.
365 **Takwi, A. and Li, Y.** (2009). The p53 Pathway Encounters the MicroRNA World. *Curr*
366 *Genomics* **10**, 194-7.
367 **Thomas, S. E., Malzer, E., Ordonez, A., Dalton, L. E., van, T. W. E. F. A., Liniker, E., Crowther,**
368 **D. C., Lomas, D. A. and Marciniak, S. J.** (2013). p53 and translation attenuation regulate distinct cell
369 cycle checkpoints during endoplasmic reticulum (ER) stress. *J Biol Chem* **288**, 7606-7617.
370 **Ungewitter, E. and Scrable, H.** (2010). Delta40p53 controls the switch from pluripotency to
371 differentiation by regulating IGF signaling in ESCs. *Genes Dev* **24**, 2408-19.
372 **Vieler, M. and Sanyal, S.** (2018). p53 Isoforms and Their Implications in Cancer. *Cancers*
373 *(Basel)* **10**.
374 **Xu, F., Wang, Y., Ling, Y., Zhou, C., Wang, H., Teschendorff, A. E., Zhao, Y., Zhao, H., He, Y.,**
375 **Zhang, G. et al.** (2022). dbDEMC 3.0: Functional Exploration of Differentially Expressed miRNAs in
376 Cancers of Human and Model Organisms. *Genomics, Proteomics & Bioinformatics*.
377 **Ye, J., Liu, P., Li, R., Liu, H., Pei, W., Ma, C., Shen, B., Zhao, D. and Chen, X.** (2022).
378 Biomarkers of connective tissue disease-associated interstitial lung disease in bronchoalveolar

379 lavage fluid: A label-free mass spectrometry-based relative quantification study. *J Clin Lab Anal* **36**,
380 e24367.
381 **Zhang, L., Liao, Y. and Tang, L.** (2019). MicroRNA-34 family: a potential tumor suppressor
382 and therapeutic candidate in cancer. *Journal of Experimental & Clinical Cancer Research* **38**, 53.
383 **Zhang, X., Groen, K., Morten, B. C., Steffens Reinhardt, L., Campbell, H. G., Braithwaite, A.**
384 **W., Bourdon, J. C. and Avery-Kiejda, K. A.** (2022). Effect of p53 and its N-terminally truncated
385 isoform, Delta40p53, on breast cancer migration and invasion. *Mol Oncol* **16**, 447-465.

386 **FIGURE LEGENDS**

387 **Figure 1. Regulation of miRNA expression by p53 and its isoform Δ40p53**

388 (A) Schematic of constructs used in study (B) Experimental setup prior to RNA sequencing.
389 (C) Western blot analysis of cell extracts from H1299 cells expressing control, p53 only,
390 Δ40p53 only and 14A construct, probed with CM1 after 48 h. (D) The cluster of differentially
391 expressed miRNAs obtained from the small RNA sequencing data set. (E) The compressed
392 cluster of significant differentially expressed miRNAs with p-value $\leq$ 0.05 (generated using
393 Heatmapper).

394 **Figure 2. Selection and validation of miRNAs for further studies**

395 (A) Western blot analysis of cell extracts from H1299 cells expressing control, p53 only,
396 Δ40p53 only and 14A construct, probed with CM1 after 48 h. (B-E) Quantitative PCR for
397 validation of miR-4671-5p, miR-34a-5p, miR-548ae-5p, miR-301b-5p, respectively, in H1299
398 cells expressing control, p53 only, Δ40p53 only and 14A construct. (F) Table for comparative
399 analysis of fold changes obtained in sequencing versus validation result. (G) Western blot
400 analysis of cell extracts from HCT116+/+ and HCT116-/-cells probed with CM1. (H)
401 Quantitative PCR for validations of miR-4671-5p, miR-34a-5p and miR-548ae-5p in
402 HCT116+/+ and HCT116-/-cells. (I) Quantitative PCR of miR-4671-5p, miR-34a-5p and miR-
403 548ae-5p in HCT116+/+ cells transfected with si p53 (30nM) and non-specific si (si Nsp). (J)
404 Western blot analysis of cell extracts from HCT116+/+ cells transfected with either si p53
405 (30nM) and non-specific si (si Nsp), probed with CM1. (K) Quantitative PCR of miR-4671-
406 5p, miR-34a-5p and miR-548ae-5p in HCT116-/- cells transfected with si Δ40p53 (30nM) and
407 non-specific si (si Nsp). (L) Western blot analysis of cell extracts from HCT116-/- cells
408 transfected with siΔ40p53 (30nM) and non-specific si (si Nsp), probed with CM1 The criterion
409 for statistical significance was $p \leq 0.05$ (*) or $p \leq 0.01$ (**) or $p \leq 0.001$(***)

410 **Figure 3. Regulation of miRNAs by Δ40p53 and p53**

411 (A) Differential expression Profile of miRNAs in cancer vs. normal obtained from dbDEMC
412 3.0 database. (B) Western blot analysis of cell extracts from H1299 transfected cells with
413 different ratios of p53 and Δ40p53 probed with CM1. (C-D) Quantitative PCR of miR-34a-5p
414 and miR-4671-5p respectively in H1299 transfected with different ratios of p53 and Δ40p53.
415 (E) Table for miR-4671-5p targets selected in the study. (F-I) Kaplan-Meier estimates of
416 survival for pancreatic adenocarcinoma (F-G) and colon tumor (H-I) classified by SGSH

417 mRNA expression levels. The number of patients at risk is indicated for time increments of 12
418 or 24 months. p values were calculated using a log rank test. (J-L) Quantitative PCR of mRNA
419 targets (SGSH, CDK11B and CDK5R1) in H1299 transfected cells with different ratios of p53
420 and Δ40p53. (M) Western blot analysis of cell extracts from HCT116+/+ and HCT116-/- cells
421 probed with CM1, SGSH, CDK11B, CDK5R1 antibodies. The criterion for statistical
422 significance was $p \leq 0.05$ (*) or $p \leq 0.01$ (**) or $p \leq 0.001$(***).

423 **Figure 4. role of miR-4671-5p**

424 (A) Quantitative PCR of SGSH, CDK11B and CDK5R1 in HCT116-/- cells transfected with
425 si Δ40p53 (30nM) and non-specific si (si Nsp). (B) Western blot analysis of cell extracts from
426 HCT116-/- cells transfected with siΔ40p53 (30nM) and non-specific si (si Nsp), probed with
427 CM1. (C) Quantitative PCR of miR-4671-5p in HCT116-/- cells transfected with miR-4671-
428 5p overexpression construct. (D) Quantitative PCR of SGSH, CDK11B and CDK5R1 in
429 HCT116-/- cells transfected with miR-4671-5p overexpression construct. (E) Western blot
430 analysis of cell extracts from HCT116-/- cells transfected with siΔ40p53 (30nM) and non-
431 specific si (si Nsp), probed with CM1 and SGSH. (F) Western blot analysis of cell extracts
432 from HCT116-/- cells transfected with miR-4671-5p overexpression construct, probed with
433 SGSH. (G) Analysis of different cell cycle phases of fixed cell extracts from HCT116-/- cells
434 transfected with miR-4671-5p overexpression construct. The criterion for statistical
435 significance was $p \leq 0.05$ (*) or $p \leq 0.01$ (**) or $p \leq 0.001$(***). (H) Left (Normal condition):
436 Under physiological conditions, high levels of the p53 translational isoform Δ40p53 suppress
437 the expression of miR-4671-5p. Reduced levels of miR-4671-5p relieve its inhibitory effect on
438 SGSH, leading to elevated SGSH expression. High SGSH levels support normal cell cycle
439 progression through G1, S, G2, and M phases. Right (Pathological condition): In conditions
440 where Δ40p53 expression is low, miR-4671-5p is upregulated. Increased miR-4671-5p inhibits
441 SGSH expression, resulting in reduced SGSH levels. This suppression contributes to intra-S-
442 phase cell cycle arrest, which is associated with impaired proliferation control and poor cancer
443 prognosis.

444 **Figure S1: (Table 1)**: miR-4671-5p targets obtained from TargetScan 7.2 database and
445 miRDB. **(Table 2)**: Result of PANTHER Statistical Overrepresentation Test of "GO molecular
446 function"-terms obtained from 786 predicted miR-4671-5p targets, using all *Homo sapiens*
447 genes as reference list. FDR: False Discovery Rate. Results for FDR $P < 0.05$ reported. **(Table**
448 **3)**: Survival analysis of patients as classified by SGSH mRNA expression levels in pancreatic
449 adenocarcinoma, colon tumor, glioblastoma and neuroblastoma gene expression datasets
450 available on R2: Genomics Analysis and Visualization Platform. p-values <0.07 reported,
451 below 0.05 considered significant. Similar analysis for hsa-miR-4671-5p expression, as
452 available in the sole miRNA expression dataset on R2.

453

Figure 1

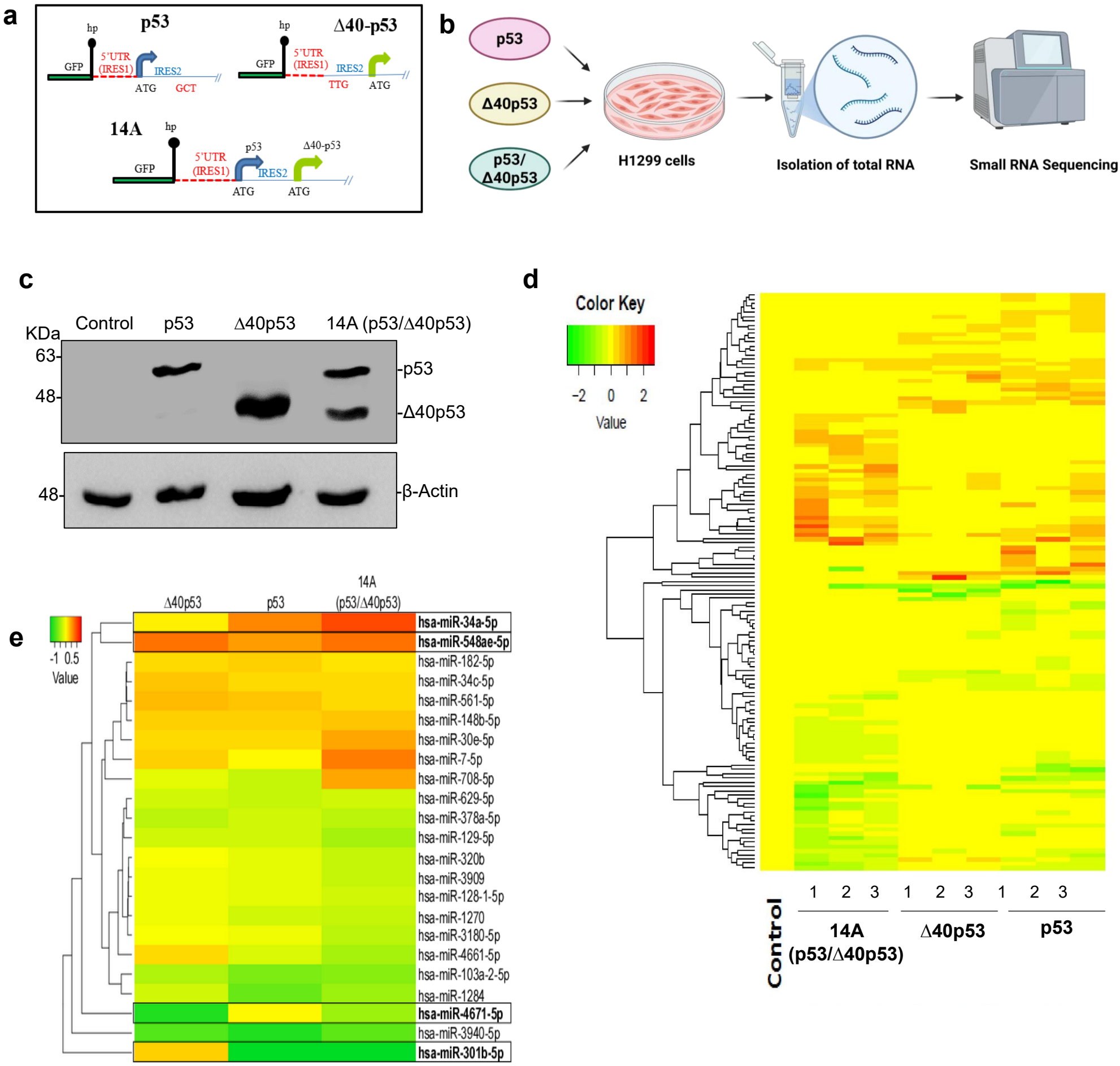
a
p53
hp
GFP
5'UTR
(IRES1)
IRES2
ATG
GCT
Δ40-p53
TTG
14A
p53
Δ40-p53
b
p53
Δ40p53
p53/
Δ40p53
H1299 cells
Isolation of total RNA
Small RNA Sequencing
c
KDa
Control
p53
Δ40p53
14A (p53/Δ40p53)
63-
48-
-p53
-Δ40p53
48-
-β-Actin
d
Color Key
-2
0
2
Value
1 2 3 1 2 3 1 2 3
Control
14A
(p53/Δ40p53)
Δ40p53
p53
e
Δ40p53
p53
14A
(p53/Δ40p53)
-1 0.5
Value
hsa-miR-34a-5p
hsa-miR-548ae-5p
hsa-miR-182-5p
hsa-miR-34c-5p
hsa-miR-561-5p
hsa-miR-148b-5p
hsa-miR-30e-5p
hsa-miR-7-5p
hsa-miR-708-5p
hsa-miR-629-5p
hsa-miR-378a-5p
hsa-miR-129-5p
hsa-miR-320b
hsa-miR-3909
hsa-miR-128-1-5p
hsa-miR-1270
hsa-miR-3180-5p
hsa-miR-4661-5p
hsa-miR-103a-2-5p
hsa-miR-1284
hsa-miR-4671-5p
hsa-miR-3940-5p
hsa-miR-301b-5p

Figure 2

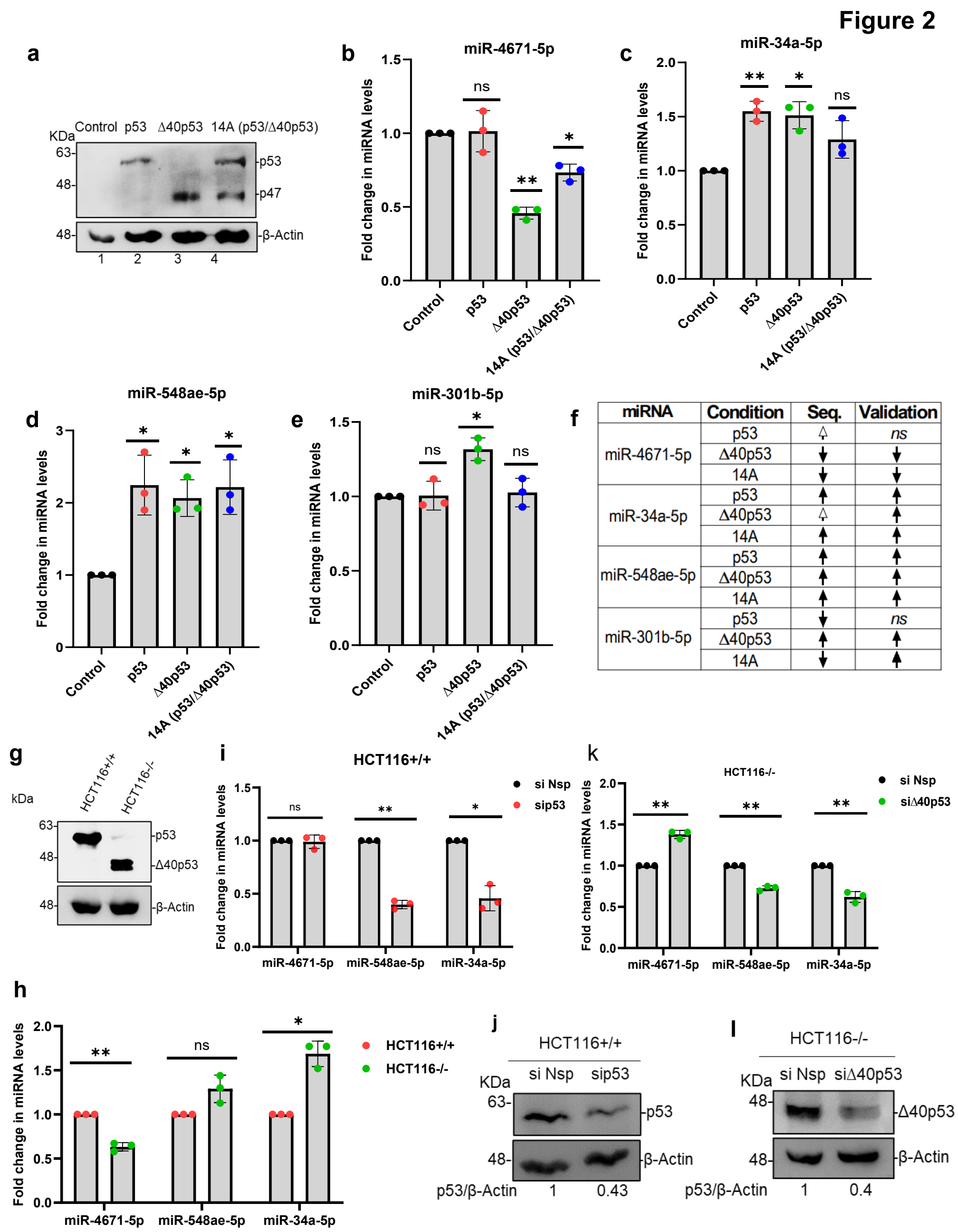

miRNA	Condition	Seq.	Validation
miR-4671-5p	p53	↑	*ns*
	Δ40p53	↓	↓
	14A	↓	↓
miR-34a-5p	p53	↑	↑
	Δ40p53	↑	↑
	14A	↑	↑
miR-548ae-5p	p53	↑	↑
	Δ40p53	↑	↑
	14A	↑	↑
miR-301b-5p	p53	↓	*ns*
	Δ40p53	↑	↑
	14A	↓	↑

Figure 3

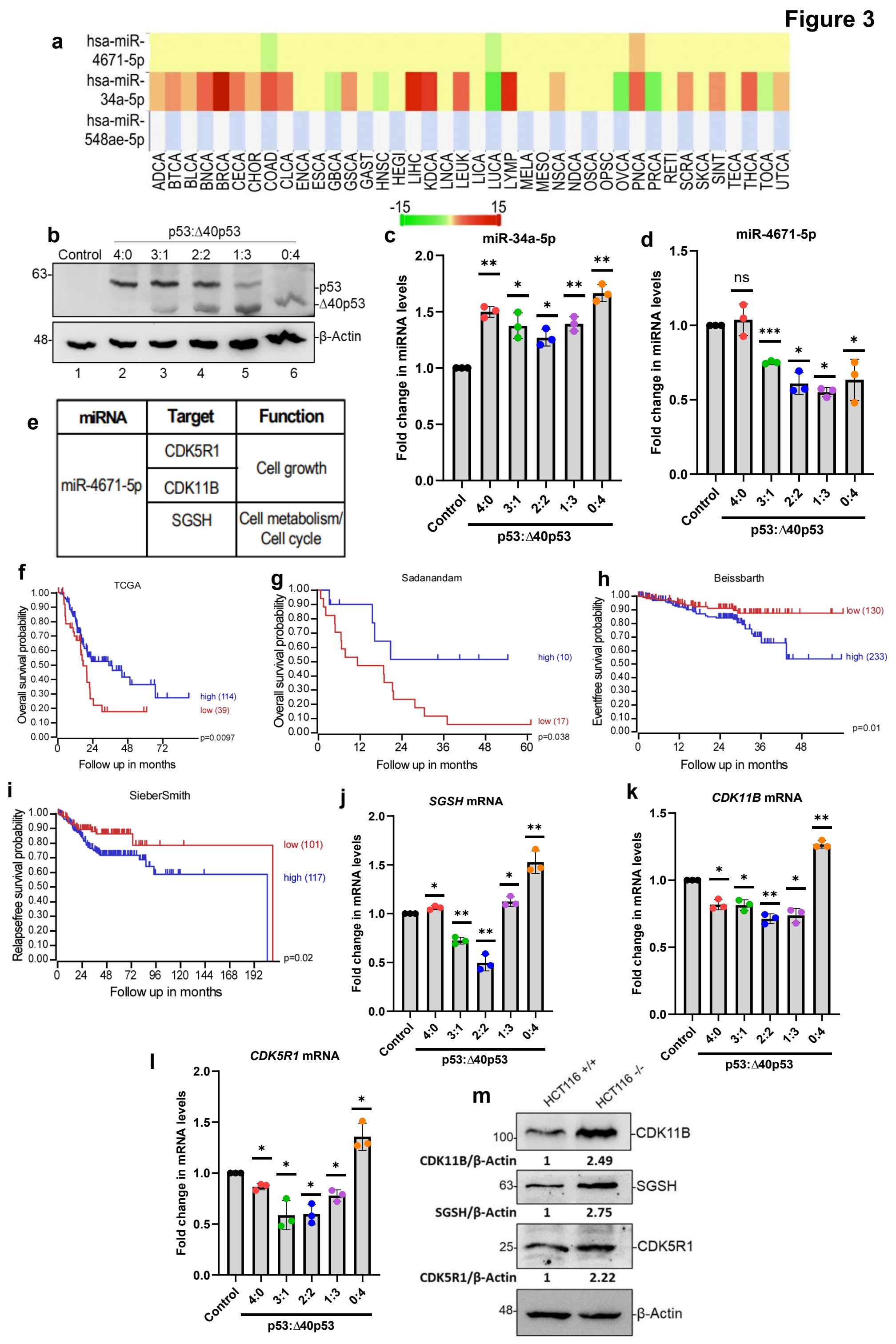
a
hsa-miR-4671-5p
hsa-miR-34a-5p
hsa-miR-548ae-5p
ADCA BTCA BLCA BNCA BRCA CECA CHOR COAD CLCA ENCA ESCA GBCA GSCA GAST HNSC HEGI LIHC KDCA LNCA LEUK LICA LUCA LYMP MELA MESO NSCA NDCA OSCA OPSC OVCA PNCA PRCA RETI SCRA SKCA SINT TECA THCA TOCA UTCA
-15
15
b
p53:Δ40p53
Control 4:0 3:1 2:2 1:3 0:4
63-
48-
p53
Δ40p53
β-Actin
1 2 3 4 5 6
c
miR-34a-5p
Fold change in miRNA levels
Control 4:0 3:1 2:2 1:3 0:4
p53:Δ40p53
d
miR-4671-5p
Fold change in miRNA levels
ns
Control 4:0 3:1 2:2 1:3 0:4
p53:Δ40p53
e
miR-4671-5p
CDK5R1
CDK11B
Cell growth
SGSH
Cell metabolism/ Cell cycle
f
TCGA
Overall survival probability
high (114)
low (39)
p=0.0097
Follow up in months
g
Sadanandam
Overall survival probability
high (10)
low (17)
p=0.038
Follow up in months
h
Beissbarth
Eventfree survival probability
low (130)
high (233)
p=0.01
Follow up in months
i
SieberSmith
Relapsefree survival probability
low (101)
high (117)
p=0.02
Follow up in months
j
SGSH mRNA
Fold change in mRNA levels
Control 4:0 3:1 2:2 1:3 0:4
p53:Δ40p53
k
CDK11B mRNA
Fold change in mRNA levels
Control 4:0 3:1 2:2 1:3 0:4
p53:Δ40p53
l
CDK5R1 mRNA
Fold change in mRNA levels
Control 4:0 3:1 2:2 1:3 0:4
p53:Δ40p53
m
HCT116 +/+
HCT116 -/-
100-
CDK11B
CDK11B/β-Actin 1 2.49
63-
SGSH
SGSH/β-Actin 1 2.75
25-
CDK5R1
CDK5R1/β-Actin 1 2.22
48-
β-Actin

Figure 4

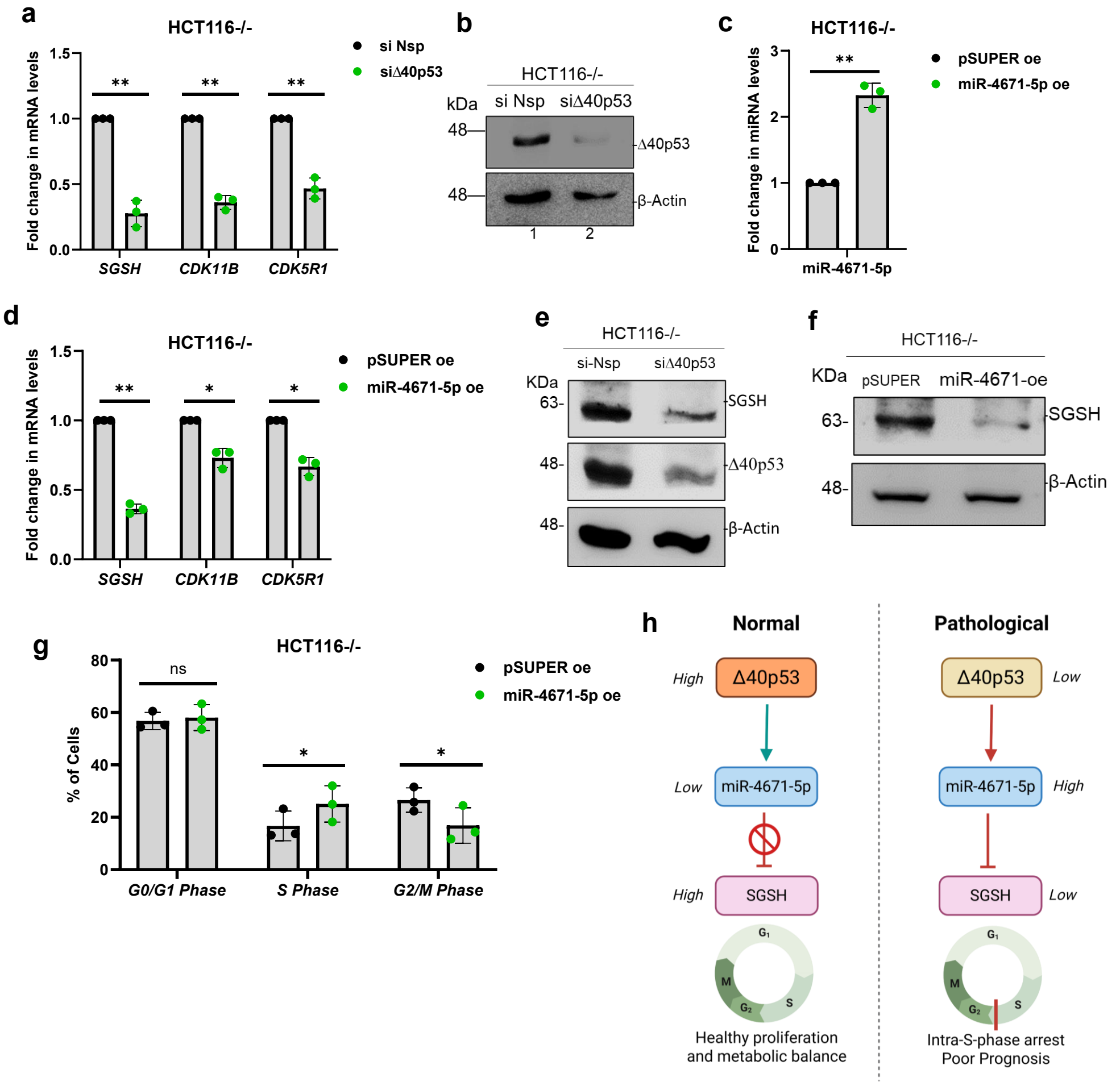
a
HCT116-/-
si Nsp
siΔ40p53
Fold change in mRNA levels
1.5
1.0
0.5
0.0
**
**
**
SGSH
CDK11B
CDK5R1
b
HCT116-/-
si Nsp
siΔ40p53
kDa
48
48
Δ40p53
β-Actin
1
2
c
HCT116-/-
pSUPER oe
miR-4671-5p oe
Fold change in miRNA levels
3
2
1
0
**
miR-4671-5p
d
HCT116-/-
pSUPER oe
miR-4671-5p oe
Fold change in mRNA levels
1.5
1.0
0.5
0.0
**
*
*
SGSH
CDK11B
CDK5R1
e
HCT116-/-
si-Nsp
siΔ40p53
KDa
63-
48-
48-
SGSH
Δ40p53
β-Actin
f
HCT116-/-
KDa
pSUPER
miR-4671-oe
63-
48-
SGSH
β-Actin
g
HCT116-/-
pSUPER oe
miR-4671-5p oe
% of Cells
80
60
40
20
0
ns
*
*
G0/G1 Phase
S Phase
G2/M Phase
h
Normal
Pathological
High
Δ40p53
Low
Δ40p53
Low
miR-4671-5p
High
miR-4671-5p
High
SGSH
Low
SGSH
G1
M
G2
S
Healthy proliferation
and metabolic balance
Intra-S-phase arrest
Poor Prognosis

Figure S1

TABLE 1

Database / miRNA	Target Scan database	miRDB
	Number of targets	Number of targets
miR-4671-5p	780	46

TABLE 2

"GO molecular function complete" terms	*Homo sapiens* (REF) # genes	hsa-miR-4671-5p target list # genes	Expected # genes	Fold Enrichment	+/-	raw P value	FDR
protein serine kinase activity	364	32	13.67	2.34	+	2.77E-05	2.30E-02
protein serine/threonine kinase activity	433	35	16.26	2.15	+	7.52E-05	4.16E-02
molecular adaptor activity	488	38	18.32	2.07	+	7.07E-05	4.40E-02
ion binding	6088	283	228.57	1.24	+	3.63E-05	2.58E-02
binding	16594	694	623.01	1.11	+	1.01E-11	5.01E-08
protein binding	14448	618	542.44	1.14	+	1.83E-09	4.56E-06
Unclassified	2297	44	86.24	0.51	-	2.92E-07	3.64E-04
olfactory receptor activity	441	2	16.56	0.12	-	2.54E-05	2.53E-02

Figure S1

TABLE 3

			p values				
Cancer/tumor	**Dataset**	**SGSH level (is poor)**	**Scan (low/high)**	**Median (Low/high)**	**Q1 v Rest (Low/high)**	**Rest v Q4 (Low/high)**	**Q1 v Q4 (Low/high)**
Mixed Pancreatic Adenocarcinoma	tcga	LOW	2.8e-03 (38/115)		9.7 e-03 (39/114)		
Mixed Pancreatic Adenocarcinoma	tcga	LOW	3.1e-05 (8/138)				
Mixed Tumor Pancreas (Exon)	Zhang	HIGH	0.035 (73/17)				
Mixed Pancreatic	Sadanandam	LOW	0.038 (17/10)				
Mixed colon adenocarcinoma	TCGA	HIGH	0.0195 (32/123)				
Mixed colon adenocarcinoma (2022-v32)	TCGA	HIGH	0.026 (29/437)				
Tumor colon	Sieber	HIGH	0.023 (181/45)				
Tumor colon	SieberSmith	HIGH	0.059 (116/170)				
Tumor colon	Smith	HIGH**	0.011 (98/134)	0.031 (117/115)			
Tumor colon	Sveen	HIGH	3.1e-03 (20/300)				
Tumor colon	Beissbarth	HIGH	0.01 (130/233)				
Tumor colon	Beauchamp	LOW	0.012 (53/103)				
Tumor colon	Tsunoda	HIGH	5.0e-03 (78/11)				
Tumor colon	Marisa	HIGH	1.1e-03(539/18)			0.061 (418/139)	
Tumor colon	SieberSmith	HIGH	0.02 (101/177)				
Tumor glioblastoma	TCGA	HIGH	4.0e-03 (58/106)				
Tumor glioblastoma	TCGA	HIGH	5.8e-04 (12/365)	0.021 (189/188)	0.012 (95/282)		0.051 (95/95)
Tumor glioblastoma	TCGA	HIGH	2.3e-04 (18/486)	1.6e-03 (253/251)	3.0e-03 (127/377)		3.8e-03 (127/127)
Tumor Neuroblastoma	Kocak	LOW	7.1e-12 (141/335)	3.9e-08 (239/237)	1.6e-08 (120/356)	1.8 e-04 (357/119)	6.4e-08 (120/120)
Tumor Neuroblastoma	Maris	LOW	7.6e-03 (68/33)			0.022 (76/25)	0.039 (26/26)
Tumor Neuroblastoma	SEQC	LOW	3.0e-17 (184/314)	2.3e-11 (249/249)	5.5e-12 (125/373)	5.0e-06 (374/124)	2.3e-11 (125/125)
Tumor Neuroblastoma	NRC	LOW	4.4e-05 (60/223)	1.1e-03 (142/141)	5.8e-04 (71/212)	5.8e-03 (213/70)	2.4e-04 (71/71)
Tumor Neuroblastoma	Asgharzadeh	LOW	0.016 (111/136)	0.042 (124/123)			
Tumor Neuroblastoma	Cangelosi	LOW	1.9e-16 (303/483)	1.6e-12 (393/393)	9.4e-12 (197/589)	3.6 e-06 (590/196)	9.0 e-12 (197/197)
Tumor Neuroblastoma	Seeger	LOW	1.1e-03 (25/77)		3.2e-03 (26/76)		0.019 (26/26)
Tumor Neuroblastoma	Versteeg	LOW	0.054 (47/41)				
Tumor Neuroblastoma	Westermann	LOW	9.1e-05 (68/71)	4.4e-04 (70/69)		0.015 (105/34)	
			p values				
Cancer/tumor	**Dataset**	**hsa-miR-4671-5p (is poor)**	**Scan (low/high)**	**Median (Low/high)**	**Q1 v Rest (Low/high)**	**Rest v Q4 (Low/high)**	**Q1 v Q4 (Low/high)**
Tumor Neuroblastoma	Bell	HIGH	0.058 (79/16)				